RSC Advances

CdSe QDs @ UIO-66 composite with enhanced photocatalytic activity towards RhB degradation under visible-light irradiation

Journal:	*RSC Advances*
Manuscript ID	RA-ART-11-2015-023565.R1
Article Type:	Paper
Date Submitted by the Author:	18-Dec-2015
Complete List of Authors:	Gan, Haijun; Changchun University of Technology, School of Chemical Engineering Wang, Zhen; Changchun University of Technology, School of Chemical Engineering Li, Huimin; Changchun University of Technology, School of Chemical Engineering Wang, Yuan-rui; Changchun University of Technology, School of Chemical Engineering Sun, Linping; Changchun University of Technology, School of Chemical Engineering Li, Ya-feng; Changchun University of Technology, School of Chemical Engineering
Subject area & keyword:	Photocatalysis < Catalysis

CdSe QDs @ UIO-66 composite with enhanced photocatalytic activity towards RhB degradation under visible-light irradiation

Haijun Gan, Zhen Wang, Huimin, Li, Yuanrui Wang, Linping Sun, Yafeng Li*

School of Chemical Engineering, Changchun University of Technology, 130012, Changchun, P. R. China

Fax: 86-0431-85716785

E-mail: liyafeng@ccut.edu.cn

Abstract: In this paper, CdSe QDs @ UIO-66 composite has been prepared and characterized by PXRD, ICP-AES, UV-visible DRS, BET and TEM. The results show that CdSe QDs are embedded into UIO-66 with high content, small size and high dispersity. The growth of CdSe QDs displays the process from interior to exterior of UIO-66 and the major of generated CdSe QDs is embedded into UIO-66. The photocatalysis of CdSe QDs @ UIO-66 composite to RhB under visible-light irradiation shows that coupling semiconductor CdSe QDs and semiconductor UIO-66 apparently enhances the photocatalytic activity and photocatalytic activity is closely related with CdSe QDs content. The photocatalytic stability indicates that the structure of CdSe QDs @ UIO-66 composite is unchangful after reacted and CdSe QDs @ UIO-66 composite can be reused several times. The photocatalytic mechanism exhibits that $O_2^{-\cdot}$ species is responsible for the photocatalytic activity.

Keywords: CdSe quantum dot; UIO-66; nanocomposite; photocatalysis; visible-light irradiation

1. Introduction

To explore and design the highly efficient photocatalyst can afford an effective and green approach for direct utilization of solar energy to drive chemical reactions [1,2]. As an important member of II-VI semiconductor family, CdSe has been largely studied as the photocatalyst of water-splitting and pollutant treatment because the adsorption band of CdSe can extend to 720nm (Eg = ~1.7eV) which almost covers the whole visible-light spectra [3,4]. The other feature of CdSe is size-dependent electronic and optical properties [5]. However, with diminishing the size of CdSe, photogenerated electron and hole are fast recombined and CdSe is easily photo-oxided. One solution is to couple the second semiconductor with an appropriate band gap to construct the core-shell structure [6,7]. In core-shell structure, the band gap of the second semiconductor spans both conduction band and valence band of CdSe. Hence, coupling CdSe and the second semiconductor can effectively improve the separation rate of photogenerated electron and hole of core-shell structure by cutting off electron-hole recombination as well as enhance the stability of the CdSe against photo-oxidation [8-10].

In the past decades, more efforts have been devoted to a kind of porous material called as the MOF (Metal-organic framework) built up from the cation/cationic cluster as the node and bi-dentate/multi-dentate organic ligand as the linker [11, 12]. MOFs have exhibited extensive applications in the fields of gas-separation/gas-storage, catalysis, drug delivery, chemical sensor and water recovery and so forth owing to designable and tunable channel, high crystallinity, large surface area, extraordinary thermal stability and chemical stability [13-18]. By far, MOFs are being enlarged continuously owing to the diversities of structures and organic ligands. Among these, UIO-66 and UIO-66 analogies which are constructed form the $Zr_6(OH)_4O_4(CO_2)_{12}$ cluster, attracts more attentions due to the extraordinarily chemical stability [19]. Especially, UIO-66 is capable to maintain the structure in the water for several months [20, 21].

UIO-66 and UIO-66 analogies, associated with large surface area and superior stability to water, not only possesses the cage-like structure to accommodate the

nanoparticle and large surface area to disperse the entrapped nanoparticle but also serves as the semiconductor material itself [22]. Therefore, UIO-66 and UIO-66 analogies are becoming potential candidates as the photocatalyst. Up to date, photocatalyst-UIO-66 composites have been prepared, such as CdS-UIO-66(NH_2), CdS-UIO-66, CdS-RGO-UIO-66, AgI-UIO-66, Ag_2CO_3-UIO-66, and CdS-MIL-101 etc.[23-28].

Several approaches have been attempted to fabricate the M or MxNy NPs@MOF composite [29]. One method is through heat treatment, such as the liquid-impregnation or gas-infiltration or even in situ sovlothermal synthesis [30-33]. The alternative method under room temperature is called as directing self-assemble or templated method [34, 35]. Comparably, the lower temperature is more favored. However, M or MxNy NPs embedded into MOF by directing self-assemble are large size or need to be capped by surfactant to avoid the aggregate of nanoparticles, which is apparently unfavorable for photocatalysis. As the hydrated UIO-66 or UIO-66 analogies is capable of attracting the anion, AgI-UIO-66 [25] and Ag_2CO_3-UIO-66 [26] with excellently photocatalytic activity have been prepared on the UIO-66 by introducing the cation Ag^+ to the solution dissolving anion I^- or HCO_3^-. However, AgI or Ag_2CO_3 prepared by this method is hugely gathered and low dispersity. In this paper, with respect to attracting both anion and cation, we have prepared the CdSe QDs @ UIO-66 composite with small size below ~10nm and high dispersity by leading H_2Se gas to the solution dissolving cation Cd^{2+} and furthermore investigated the photocatalytic performance to RhB.

2. EXPERIMENTAL SECTIONS

2.1. Synthesis and Characterization

2.1.1. Synthesis

UIO-66. UIO-66 was synthesized according to our previous work [36]. Typically, $ZrCl_4$ (150mg, 0.644mmol) was dissolved into solution of acetic acid (5ml, 87.36mmol)/DMF (40ml, 516mmol) to clear solution and continuously stirred for half an hour. Then, BDC (120mg, 0.723mmol) was dissolved into the solution. Finally, the

mixed solution with molar ratio of DMF : HAc : BDC : $ZrCl_4$ = 800 : 135 : 1.12 : 1 was put into the microwave oven and irradiated at 100°C for 2 hours. The product was centrifuged at 6000rpm for 5min, washed three times by ethanol and dried at 60°C overnight.

CdSe QDs @ UIO-66. 50mg of activated UIO-66 and 45.6mg (0.2mmol) of $CdCl_2 \cdot 2.5H_2O$ were successively added into 10ml ethanol to obtain the suspended solution (1). Then, the suspended solution (1) purged the oxygen with N_2 for 0.5hr to restrain the oxidation of H_2Se. The colorless NaHSe/ethanol solution (2) was prepared by reacting 15.8mg (0.2mmol) of Se and 15.1mg (0.4mmol) of $NaBH_4$ in ethanol solution at 50°C for 0.5hr under N_2 protection. Afterwards, 1mol/L H_2SO_4 was slowly dropped into solution (2) to produce H_2Se. The H_2Se gas was transferred into suspended solution (1) with N_2 as carrier. After reaction was ended, the product was centrifugally isolated at 5000rpm and washed three times using ethanol by the method of disperse and centrifugation. The black-red product (denoted as CdSe QDs @ UIO-66-0.2) was vacuumedly dried at 60°C.

CdSe QDs @ UIO-66-0.05, CdSe QDs @ UIO-66-0.1 and CdSe QDs @ UIO-66-0.4 were successively prepared according to the above process.

2.1.2 Characterization Techniques

Powder X-ray diffraction (PXRD) patterns were recorded on a Rigaku D/MAX PC2200 diffractometer for Cu Kα radiation (λ =1.5406 Å), with a scan speed of 5°/min.

The morphologies and size of the samples were inspected on a transmission electron microscope (JEOL-2000ex) and HRTEM (Tecnai G2 F20S-Twin).

N_2 isothermal adsorption experiments were performed at 77 K with TriStar II 3020 (Micromeritics Instrument Corporation) apparatus using nitrogen as the probing gas. The samples were vacuumed for 10hrs at 75°C before the data were collected.

The CdSe content was determinated by IRIS Intrepid II ICP instrument (Thermo Electron Corp.). The CdSe QDs @ UIO-66 was dissolved by the H_2SO_4/H_2O_2 and diluted to a certain concentration.

UV-Vis spectra were recorded at UV-1901 spectrometer (Youke, China).

The UV-visible diffuse reflectance spectra (DRS, taking $BaSO_4$ as internal reference sample) were performed on the dry-pressed disk samples using a Hitachi U-3900 spectrophotometer equipped with an integrating sphere assembly.

2.2 photocatalytic degradation of CdSe QDs @ UIO-66-0.2 to RhB

The activity of the catalyst was evaluated by measuring the absorbance of the RhB solution at 554 nm during the dye degradation. For the degradation experiment with CdSe QDs @ UIO-66-0.2, the sample (15 mg) was mixed with an aqueous solution of RhB (20 mL, 0.02 mmol/L) in a 50 mL round-bottomed flask. The solution pH was adjusted to 2~3 with 1mol/L HCl. The mixture was first stirred with a magnetic stirrer in the dark for 1 hr to reach complete adsorption equilibrium. Thereafter, the suspension was irradiated by a 500 W halogen lamp. A 420 nm cutoff filter were placed between the sample and the light source to eliminate the UV and infrared irradiation. During the whole process, the solids were kept in suspension by magnetic stirring and air was continuously bubbled through the reaction mixture at a rate of 20 mL/min to maintain dissolved oxygen content. At every 10min intervals, 1 mL aliquots were sampled and centrifuged. The dye concentration of the clear supernatant was then measured with a UV-1901 UV/Vis spectrometer. For the degradation experiment with CdSe QDs @ UIO-66-0.05, CdSe QDs @ UIO-66-0.1, CdSe QDs @ UIO-66-0.4, and the control experiment, all conditions were the same as those in the experiment with CdSe QDs @ UIO-66-0.2. In the control experiment, the mechanical mixture of UiO-66 and CdSe QDs were added to the RhB solution, and the amount of pristine UiO-66 or CdSe QDs was equal to the actual amount of that in CdSe QDs @ UIO-66-0.2. The blank experiments were also handled under the same conditions, but no catalyst was added.

3. Results and Discussions

3.1Material characterization

The crystal phase of CdSe QDs and CdSe QDs @ UIO-66 are determined by PXRD pattern. From Fig.1c, diffraction peak positions of as-synthesized CdSe

matches those of cubic phase CdSe (2θ=25.3°, 42°, 49.7°). The diffraction peaks of as-synthesized nanoparticle CdSe are obviously broadened and weakened, meaning that the particle size of CdSe is very small. From Fig.1d-1g, with CdSe content in UIO-66 inclining, the diffraction peak at 25.3° gradually becomes strong. This indicates that the structure of CdSe QDs in UIO-66 may be assigned to the cubic phase. The peak positions of UIO-66 in CdSe QDs @ UIO-66 are coincided with simulated UIO-66, and meantime intensity of UIO-66 loaded by CdSe QDs is basically unchangeful and still very strong.

The catalytic activity of catalyst is proportional with the amount of active species. Therefore, Cd and Se element contents in CdSe QDs @ UIO-66 are acquired by ICP-AES, respectively (Table 1). The CdSe contents in CdSe QDs @ UIO-66 are calculated by determined Cd and Se contents, respectively. CdSe QDs amount calculated by Cd is slightly higher than one calculated by Se because the small amount of Cd may be left on CdSe QDs @ UIO-66 composites. As the $CdCl_2$ amount increases, the increment of CdSe content in CdSe QDs @ UIO-66 decreases and at the meantime the deviation between experimental and theoretical CdSe content gradually becomes large. Hence, CdSe QDs @ UIO-66-0.2 is employed for further photocatalysis to RhB.

Fig.1

Table 1 CdSe content, Langmuir surface area and pore volume of CdSe QDs @ UIO-66 samples

sample	CdSe contenet calculated by Cd	CdSe content calculated by Se	Theoretical value (%)	Langmuir surface area (m^2/g)	Total pore volume (cm^3/g)
UIO-66	-	-	-	1835.8(100%)	0.55
CdSe@UIO-66-0.05	15.1%	13.6%	16.1%	1392.2(-24%)	0.44
CdSe@UIO-66-0.1	23.2%	20.5%	27.5%	1206.0(-34%)	0.35
CdSe@UIO-66-0.2	32.3%	29.4%	43.1%	1070.9(-42%)	0.27
CdSe@UIO-66-0.4	38.3%	35.5%	60.2%	844.6(-54%)	0.17

The size of CdSe QDs embedded in UIO-66 plays an important role in photocatalysis because activity of CdSe QDs is size-dependent. At low amount of $CdCl_2$, CdSe QDs are basically encapsulated in UIO-66 (Fig.2(A)). With increasing the amount of $CdCl_2$, CdSe QDs begin to emerge, further expand and finally tend to be saturated on the surface of UIO-66 (Fig.2(B)-(D)). Nevertheless, CdSe QDs on the outer surface of UIO-66 is obviously small size below 10nm. The morphology of UIO-66 is unchangeful after be loaded by the CdSe QDs**.** HRTEM images of CdSe QDs @ UIO-66-0.2 confirm the size of CdSe QDs and give rise to lattice fringes of CdSe QDs (Fig.3). The lattice fringe of CdSe QDs is about 0.35nm, which consists with the *d* value of (111) face (2θ=25.3°) of cubic phase. In Fig.3(A), there are two typical zones: (i) zone A represents the interior grown CdSe QDs; (ii) zone B stands for the exterior grown CdSe QDs. In zone A (Fig.3(B)), there clearly exists CdSe QDs in UIO-66 constructed just by several lattice fringes. Although there exists CdSe QDs aggregate, size of CdSe QDs is only about several nanometer. In zone B (Fig.3(C)), the size of CdSe QD is apparently bigger than that in zone A, while the CdSe QDs aggregate badly.

Fig.2

Fig.3

The dispersity of active species in catalyst is associated with the surface area which the active site is proportional with. The surface areas of pristine UiO-66 and the CdSe QDs @ UIO-66 composites are calculated by N_2 isothermal adsorption at 77K. The adsorption/desorption isotherms are shown in Fig.S1 of Supporting Information, and the corresponding results are listed in Table 1. The surface areas of samples decrease with CdSe content in CdSe QDs @ UIO-66 increasing. Because the excessive CdSe QDs would go into solution rather than on UIO-66 with increasing the CdSe amount, CdSe QDs @ UIO-66-0.2 is employed for further photocatalysis to RhB. In case of CdSe QDs @ UIO-66-0.2, the surface area decreases about 42% with CdSe QDs content of 32.3%, manifesting the dispersity of CdSe QDs.

The absorption spectrum of CdSe QDs @ UIO-66 is investigated by the UV/Vis

diffuse reflectance spectra. As shown in Fig.4, absorption edge of pristine CdSe is at about 720 nm, which contains the whole visible spectral range. However, pristine UiO-66 is transparent between 350 and 800 nm, so that it can only be excited by UV light. All the CdSe QDs @ UIO-66 composites have an absorption edge at about 710 nm, indicating that these samples all possess good visible-light absorption ability. The bandgap energies (Eg) of these samples are speculated from the spectra. According to Fig.S2 in Supporting Information, the Eg of pristine CdSe and UiO-66 are about 1.87 and 3.81 eV. The bandgaps Eg of all the CdSe QDs @ UIO-66 composites are around 1.91 eV.

Fig.4

3.2 CdSe QDs @ UIO-66 growth mechanism

The growth of CdSe QDs in/on UIO-66 refers to three aspects: (1) content; (2) particle size; (3) dispersity, which catalytic activity is intimately associated with. From TEM (Fig.2) and HRTEM (Fig.3), CdSe QDs growth displays a process from interior to exterior of UIO-66 with increasing the amount of $CdCl_2$. This process can be described as adsorption, diffusion and deposition. The adsorption amount of UIO-66 vs. Cd^{2+} ion under the different concentration is acquired by the ICP-AES and listed in Table 2. From Table 2, although the adsorption amount increases with increasing the amount of $CdCl_2 \cdot 2.5H_2O$, the adsorption rate of UIO-66 vs. Cd^{2+} ion basically is kept at ~20%. The concentration of Cd^{2+} ion in UIO-66 is higher than that on UIO-66 because the activated UIO-66 prefers to absorb the water and generate the hydroxyl group which can attract the Cd^{2+} ion. Therefore, CdSe would grow preferentially in UIO-66 close to the interface as the low-concentration H_2Se diffuses into UIO-66 and combines high-concentration Cd^{2+} ion to be deposited in UIO-66. As CdSe content increases, interior growth rate of CdSe decreases because the generated CdSe impedes the further diffusion of H_2Se. Subsequently, CdSe QDs would go on growing on outer surface of UIO-66. While $CdCl_2$ amount is further added, the growth of CdSe QDs on UIO-66 becomes slow and CdSe QDs begin to aggregate. Meanwhile, the major of subsequently generated CdSe QDs go into solution rather

than on UIO-66. Notably, we speculate that the major of CdSe QDs is embedded into UIO-66 rather than on the surface of UIO-66.

Table 2 The adsorption amount of UIO-66 vs. Cd^{2+} ion under the different concentration

Added amount of $CdCl_2 \cdot 2.5H_2O$/mg	11.5	23	46	92
Cd^{2+} adsorption amount(mg)/50mgUIO-66	1.21	2. 75	4.25	8.58

3.3 Photocatalysis activity

The photocatalysis activities of samples are investigated by the degradation ability towards RhB under visible-light irradiation (Fig.5). To verify the synergism of CdSe and UIO-66, a mechanical mixture of CdSe and UIO-66 containing the equal amount of CdSe with that of CdSe QDs @ UIO-66-0.2 is used to the photocatalysis degradation of RhB. A blank experiment without any catalyst is done under the same conditions. In absence of catalyst (blank experiment), RhB hardly occurs to degrade under the visible-light irradiating. In presence of catalyst, all catalysts can degrade the RhB under the visible-light irradiating. In the presence of CdSe QDs @ UIO-66-0.1, CdSe QDs @ UIO-66-0.2, CdSe QDs @ UIO-66-0.4, RhB has been completely degraded after irradiated by the visible light in 50min. In the case of CdSe QDs @ UIO-66-0.05, RhB is degraded about 80% under the same condition, meaning that the CdSe amount may be not adequate enough to catalyze RhB. For a mechanical mixture of CdSe and UIO-66, the photocatalytic activity is close to that of CdSe QDs @ UIO-66-0.05 and apparently lower than that of CdSe QDs @ UIO-66-0.2 which has the same CdSe content. This shows that the synergism between CdSe and UIO-66 enhances photocatalytic degradation of RhB.

Fig.5

Photocatalytic activity of CdSe QDs @ UIO-66 to RhB is mainly controlled by three factors: (1) CdSe content; (2) CdSe dispersity; (3) CdSe nanoparticle size. In this work, CdSe content is relatively a main factor. Because the major of formed CdSe

QDs is embedded into UIO-66, the dispersity and size of CdSe QDs is varied very little. With CdSe content increasing, the concentration of light-generated charge carriers which are responsible for photocatalytic activity would gradually increase. Hence, with CdSe content increasing, photocatalytic activity also increases and however photocatalytic activity is to be saturated after certain CdSe content.

3.4 Photocatalytic stability

The photocatalytic stability of CdSe QDs @ UIO-66 is evaluated by the PXRD of reacted CdSe QDs @ UIO-66. As illustrated in Fig.S4 in the Supporting information, the intensity and position of peaks between CdSe QDs @ UIO-66 and reacted CdSe QDs @ UIO-66 are basically identical, indicating the stability of CdSe QDs @ UIO-66. The stability of CdSe QDs @ UIO-66-0.2 is further studied by collecting the reacted CdSe QDs @ UIO-66 and then reusing it for another cycle (Fig.6). After every cycle, the degradation rate of RhB declines approximately about 1%, which probably arises from the loss of CdSe on the UIO-66.

Fig.6

3.5 Photocatalytic mechanism

The hydroxyl radicals ($HO^{\cdot}$), superoxide radicals ($O_2^{\cdot-}$), and holes (h^+) are the three main active species referred to photocatalytic oxidation process. To further explore the photocatalytic mechanism of RhB degradation through the CdSe QDs @ UIO-66, isopropyl alcohol (IPA), benzoquinone (BQ), and ethylenediaminetetraacetic acid (EDTA) are introduced into the degradation system to entrap $HO^{\cdot}$, $O_2^{\cdot-}$ and h^+, respectively. Fig.7 shows the effect of these scavengers as well as of N_2 purging on the photocatalytic activity of CdSe QDs @ UIO-66-0.2. The introductions of IPA and EDTA virtually have no influences on the RhB degradation rate, meaning that $HO^{\cdot}$ and h^+ are not main factors to decide the degradation rate of RhB. With the introduction of BQ, the RhB degradation rate significantly declines, which indicates that $O_2^{\cdot-}$ is the decisive factor to influence the degradation rate of RhB. This is confirmed by purging the dye solution with N_2 which can decrease the dissolved O_2.

Moreover, except for neutral condition, photogenerated $HO^{\cdot}$ is unstable in either acid or base. Hence, $O_2^{-\cdot}$ is the main factor to decide the degradation rate of RhB rather than $HO^{\cdot}$ or h^+.

Fig.7

4. Conclusion

In a sum, CdSe QDs can be embedded into UiO-66 with high content, small size and high dispersity. CdSe QDs growth displays the process from interior to exterior of UIO-66 and the major of generated CdSe QDs is embedded into UIO-66. The coupling semiconductor CdSe QDs and semiconductor UIO-66 apparently enhances the photocatalytic activity to RhB and CdSe QDs content is closely related with photocatalytic activity. The structure of reacted CdSe QDs @ UIO-66 composite and reuse of CdSe QDs @ UIO-66 composite testifies the photocatalytic stability. The photogenerated $O_2^{-\cdot}$ species is responsible for the photocatalytic activity.

Referrence

[1] (a) M. R. Hoffmann, S. T. Martin, W. Choi, D. W. Bahnemann, Chem. Rev., 1995, 95, 69; (b) S. Linic, P. Christopher, D. B. Ingram, Nat. Mater., 2011, 10, 911.

[2] (a) A. D. Paola, E. García-López, G. Marci, L. Palmisano, J. Hazard. Mater., 2012, 211-212, 3; (b) C. Chen, W. Ma, J. Zhao, Chem. Soc. Rev., 2010, 39, 4206.

[3] F. A. Frame, F. E. Osterloh, J. Phys. Chem. C, 2010, 114, 10628.

[4] L. X. Yang, S. L. Luo, R. H. Liu, Q. Y. Cai, Y. Xiao, S. H. Liu, F. Su, L. F. Wen, J. Phys. Chem. C, 2010, 114, 4783.

[5] (a) I. Robel, M. Kuno, P. V. Kama, J. Am. Chem. Soc., 2007, 129, 4136; (b) A. Kongkanand, K. Tvrdy, K. Takechi, M. Kuno, P. V., Kamat, J. Am. Chem. Soc., 2008, 130, 4007.

[6] J. H. Pan, H. Q. Dou, Z. G. Xing, C. Xu, J. Z. Ma, X. S. Zhao, J. Mater. Chem., 2010, 20, 4512.

[7] (a) C. H. Chuang, T. L. Doane, S. S. Lo, G. D. Scholes, C. Burda, ACS Nano 2011, 5, 6016; (b) K. Tvrdy, P. V. Kamat, Proc. Natl. Acad. Sci. U.S.A., 2011, 108, 29.

[8] H. Gerischer, M. Luebke, J. Electroanal. Chem., 1986, 204, 225.

[9] S. Hotchandani, P. V. Kamat, J. Phys. Chem., 1992, 96, 6834.

[10] C. Nasr, S. Hotchandani, P. V. Kamat, Proc. Ind. Acad. Sci., 1995, 107, 699.

[11] D. J. Tranchemontagne, J. L. Mendoza-Cortés, M. O'Keeffe, O. M. Yaghi, Chem. Soc. Rev., 2009, 38, 1257.

[12] M. Li, D. Li, M. O'Keeffe, O. M. Yaghi, Chem. Rev., 2014, 114, 1343.

[13] M. P. Suh, H. J. Park, T. K. Prasad, D. W. Lim, Chem. Rev., 2012, 112, 782.

[14] K. Sumida, D. L. Rogow, J. A. Mason, T. M. McDonald, E. D. Bloch, Z. R. Herm, T. H. Bae, J. R. Long, Chem. Rev., 2012, 112, 724.

[15] L. E. Kreno, K. Leong, O. K. Farha, M. Allendorf, R. P. Van Duyne, J. T. Hupp, Chem. Rev., 2012, 112, 1105

[16] P. Horcajada, R. Gref, T. Baati, P. K. Allan, G. Maurin, P. Couvreur, G. Férey, R. E. Morris, C. Serre, Chem. Rev., 2012, 112, 1232.

[17] J. Y. Lee, O. K. Farha, J. Roberts, K. A. Scheidt, S. B. T. Nguyen, J. T. Hupp, Chem. Soc. Rev., 2009, 38, 1450.

[18] A. J. Howarth, Y. Liu, J. T. Hupp, O. K. Farha, CrystEngComm., 2015, 17, 7245.

[19] J. H. Cavka, S. Jakobsen, U. Olsbye, N. Guillou, C. Lamberti, S. Bordiga and K. P. Lillerud, J. Am. Chem. Soc., 2008, 130, 13850.

[20] J. B. DeCoste, G. W. Peterson, H. Jasuja, T. G. Glover, Y. G. Huang, K. S. Walton, J. Mater. Chem. A, 2013, 1,5642.

[21] H. Furukawa, F. Gándara, Y. B. Zhang, J. C. Jiang, W. L. Queen, M. R. Hudson, O. M. Yaghi, J. Am. Chem. Soc., 2014, 136, 4369.

[22] C. G. Silva, I. Luz, F. X. Llabrés i Xamena, A. Corma, H. García, Chem. Eur. J., 2010, 16, 11133.

[23] L. Shen, S. Liang, W. Wu, R. Liang, L. Wu, J. Mater. Chem. A, 2013, 1, 11473.

[24] R. Lin, L. J. Shen, Z. Y. Ren, W. M. Wu, Y. X. Tan, H. R. Fu, J. Zhang, L. Wu, Chem. Commun., 2014, 50, 8533.

[25] Z. Sha, H. S. O. Chan, J. Wu, J. Hazard. Mater., 2015, 229, 132.

[26] Z. Sha, J. L. Sun, H. S. O. Chan, S. Jaenicke, J. Wu, ChemPlusChem., 2015, 80, 1321.

[27] J. He, Z. Y. Yan, J. Wang, J. Xie, L. Jiang, Y. Shi, F. Yuan, F. Yu, Y. Sun, Chem. Commun., 2013, 49, 6761-6763.

[28] J. Aguilera-Sigala, D. Bradshaw, Coord. Chem. Rev., 2015, in press

[29] Q. L. Zhu, Q. Xu, Chem. Soc. Rev., 2014, 43, 5468.

[30] R. Ameloot, M. B. J. Roeffaers, G. D. Cremer, F. Vermoortele, J. Hofkens, B. F. Sels, D. D. Vos, Adv. Mater., 2011, 23, 1788.

[31] S. Hermes, M. K. Schröter, R. Schmid, L. Khodeir, M. Muhler, A. Tissler, R. W. Fischer, R. A. Fischer, Angew. Chem. Int. Ed., 2005, 44, 6237.

[32] H. L. Liu, L. Chang, L. Y. Chen, Y. W. Li, J. Mater. Chem. A, 2015, 3, 8028.

[33] L. Shen, W. Wu, R. Liang, R. Lin, L. Wu, Nanoscale, 2013, 5, 9374.

[34] G. Lu, S.Z. Li, Z. Guo, O. K. Farha, B. G. Hauser, X. Y. Qi, Y. Wang, X. Wang, S. Y. Han, X. G. Liu, J. S. DuChene, H. Zhang, Q. C. Zhang, X. D. Chen, J. Ma, S. C. J. Loo, W. D. Wei, Y. H. Yang, J. T. Hupp, F. W. Huo, Nat. Chem., 2012, 4, 310.

[35] T. Tsuruoka, H. Kawasaki, H. Nawafune, K. Akamatsu, ACS Appl. Mater. Interfaces, 2011, 3, 3788.

[36] Y. F. Li, Y. Liu, W. Y. Gao, L. M. Zhang, W. Liu, J. J. Lu, Z. Wang, Y. J. Deng, CrystEngComm., 2014, 16, 7037.

Caption of figure

Fig.1 The PXRD patterns of CdSe QDs and CdSe QDs @ UIO-66. a. simulated UIO-66; b. simulated cubic-phase CdSe; c. pure CdSe QDs; d. CdSe QDs @ UIO-66-0.05; e. CdSe QDs @ UIO-66-0.1; f. CdSe QDs @ UIO-66-0.2; g. CdSe QDs @ UIO-66-0.4.

Fig.2 TEM of CdSe QDs @ UIO-66. (A) CdSe QDs @ UIO-66-0.05; (B) CdSe QDs @ UIO-66-0.1; (C) CdSe QDs @ UIO-66-0.2; (D) CdSe QDs @ UIO-66-0.2.

Fig.3 HRTEM images of CdSe QDs @ UIO-66-0.2. (A) zone A represents the interior grown CdSe QDs and zone B stands for the exterior grown CdSe QDs; (B) the size and fringes of interior grown CdSe QDs; (C) the size and fringes of exterior grown CdSe QDs.

Fig.4 UV/Vis diffuse reflectance spectra of different samples. a. UIO-66; b. CdSe; c. CdSe QDs @ UIO-66-0.05; d. CdSe QDs @ UIO-66-0.1; e. CdSe QDs @ UIO-66-0.2; f. CdSe QDs @ UIO-66-0.4.

Fig.5 Photocatalytic degradation of RhB. (■)CdSe QDs @ UIO-66-0.4; (▽)CdSe QDs @ UIO-66-0.2; (□)CdSe QDs @ UIO-66-0.1; (○) CdSe QDs @ UIO-66-0.05; (X) the control experiment; (△) the blank.

Fig.6 Reuse of CdSe QDs @ UIO-66 catalyst. (△) 1st cycle; (▽) 2^{nd} cycle; (□) 3^{rd} cycle; (○) 4^{th} cycle.

Fig.7 Effects of different scavengers and N_2 purging on the degradation of RhB by CdSe QDs @ UiO-66-0.2 under visible-light irradiation. (□) EDTA; (△) CdSe QDs @ UiO-66-0.2; (○) IPA; (▽) N_2 purging; (■) QB.

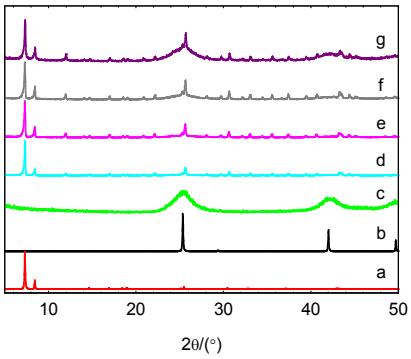

Fig.1 The PXRD patterns of CdSe QDs and CdSe QDs @ UIO-66. a. simulated UIO-66; b. simulated cubic-phase CdSe; c. pure CdSe QDs; d. CdSe QDs @ UIO-66-0.05; e. CdSe QDs @ UIO-66-0.1; f. CdSe QDs @ UIO-66-0.2; g. CdSe QDs @ UIO-66-0.4.

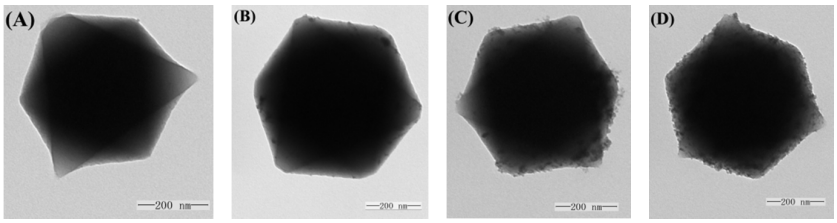

Fig.2 TEM of CdSe QDs @ UIO-66. (A) CdSe QDs @ UIO-66-0.05; (B) CdSe QDs @ UIO-66-0.1; (C) CdSe QDs @ UIO-66-0.2; (D) CdSe QDs @ UIO-66-0.2.

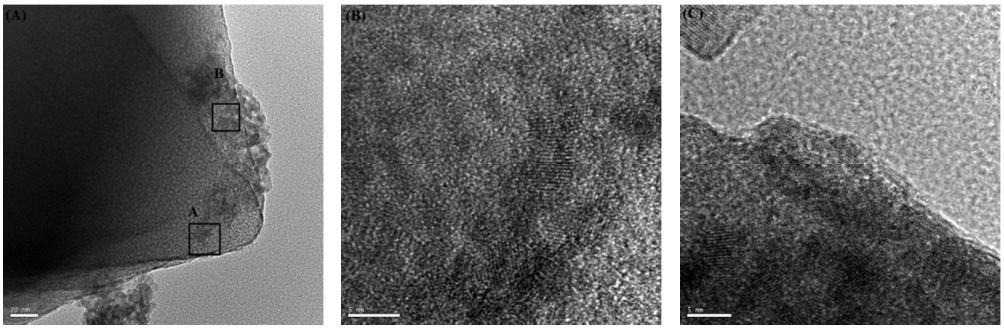

Fig.3 HRTEM images of CdSe QDs @ UIO-66-0.2. (A) zone A represents the interior grown CdSe QDs and zone B stands for the exterior grown CdSe QDs; (B) the size and fringes of interior grown CdSe QDs; (C) the size and fringes of exterior grown CdSe QDs.

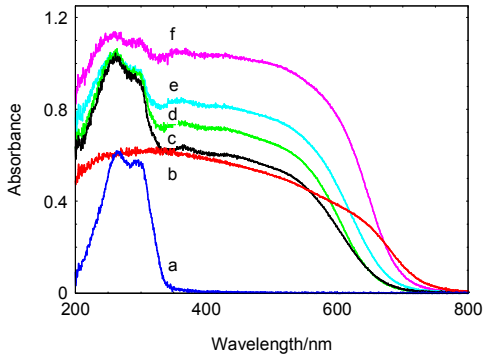

Fig.4 UV/Vis diffuse reflectance spectra of different samples. a. UIO-66; b. CdSe; c. CdSe QDs @ UIO-66-0.05; d. CdSe QDs @ UIO-66-0.1; e. CdSe QDs @ UIO-66-0.2; f. CdSe QDs @ UIO-66-0.4.

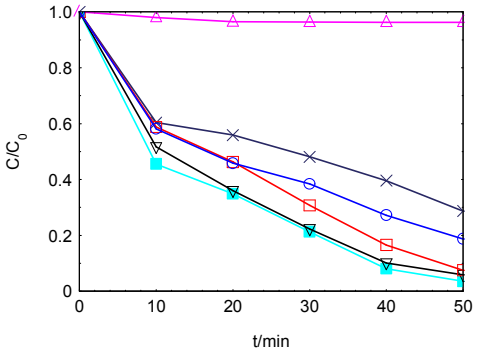

Fig.5 Photocatalytic degradation of RhB. (■)CdSe QDs @ UIO-66-0.4; (▽)CdSe QDs @ UIO-66-0.2; (□)CdSe QDs @ UIO-66-0.1; (○) CdSe QDs @ UIO-66-0.05; (X) the control experiment; (△) the blank.

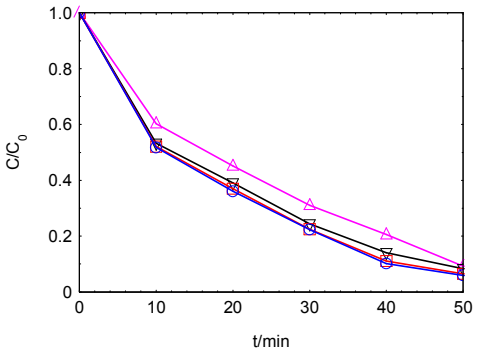

Fig.6 Reuse of CdSe QDs @ UIO-66 catalyst. (△) 1st cycle; (▽) 2nd cycle; (□) 3rd cycle; (○) 4th cycle.

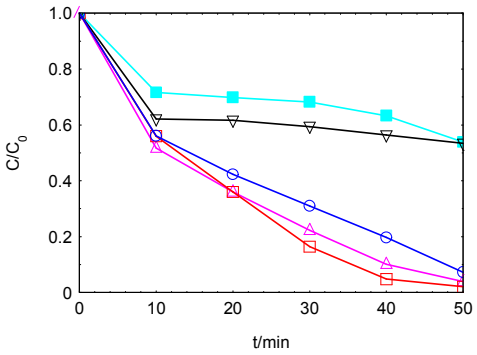

Fig.7 Effects of different scavengers and N_2 purging on the degradation of RhB by CdSe QDs @ UiO-66-0.2 under visible-light irradiation. (□) EDTA; (△) CdSe QDs @ UiO-66-0.2; (○) IPA; (▽) N_2 purging; (■) QB.

Graphic abstract

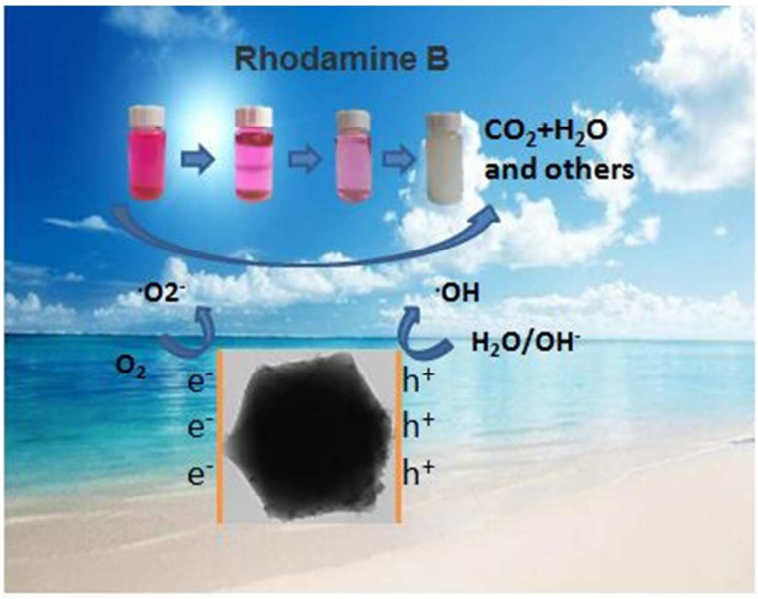

Highlight

Preparation of core-shell CdSe QDs @ UIO-66 by the method of ship-in-bottle and enhanced photocatalysis to RhB under visible-light irradiation.